Interaction strength and molecular orientation of a single layer of pentacene in organic-metal interface and organic-organic heterostructure

Mirco Chiodi and Luca Gavioli*
Dipartimento di Fisica, Università Cattolica del Sacro Cuore di Brescia, via Musei 41, I-25100 Brescia, Italy

Marco Beccari and Valeria Di Castro
Dipartimento di Chimica, Università di Roma "La Sapienza," Piazzale Aldo Moro 2, I-00185 Roma, Italy

Albano Cossaro, Luca Floreano, and Alberto Morgante
CNR-INFM Laboratorio Nazionale TASC, Basovizza SS-14, Kilometer 163.5, I-34012 Trieste, Italy

Aloke Kanjilal†
CNR-INFM Center on nanoStructures and bioSystems at Surfaces (S^3)*, Via G. Campi 213/A, I-41100 Modena, Italy*

Carlo Mariani and Maria Grazia Betti
Dipartimento di Fisica, Università di Roma "La Sapienza," Piazzale Aldo Moro 2, I-00185 Roma, Italy
(Received 28 November 2007; published 14 March 2008)

A single layer (SL) of pentacene molecules deposited on the Cu(119) surface and on an organic self-assembled monolayer (SAM) has been investigated by near-edge x-ray absorption fine structure (NEXAFS) at the C *K* edge, and by photoemission at the C 1*s* core level. The lowest unoccupied molecular orbitals (LUMOs) of the pentacene SL on the SAM are basically unaffected with respect to that of pentacene in the gas phase, indicating a weak interaction of pentacene with the SAM, while a strong redistribution of the LUMO-related final states is observed when the molecules are deposited on the Cu(119) substrate, sign of an electronic mixing between molecular and metal electronic states, in agreement with recent theoretical predictions. The strong dichroic response of the NEXAFS signal indicates upstanding pentacene molecules oriented 16° off normal for the organic-organic heterostructure. The rehybridization of pentacene orbitals with Cu states at the pentacene/Cu interface hinders an accurate determination of the molecule orientation, which is, however, compatible with molecules lying flat on the Cu(119) terraces.

DOI: 10.1103/PhysRevB.77.115321 PACS number(s): 81.07.Pr, 61.05.cj, 73.20.−r

I. INTRODUCTION

The design and construction of organic nanostructures at surfaces are topics of intense research for the advancement of nanotechnology and molecular-based devices. Organic molecules can organize into periodic arrays on well defined surfaces, forming a vast variety of molecular one-dimensional and two-dimensional superstructures and allowing for tunable anchoring sites, nanostructure orientation, and interaction strength.

Polyacenes, π-conjugated organic molecules composed of fused benzene rings, are promising candidates among molecular conductors. The control and gauge of the interaction process and the electronic properties at the organic-metal (O-M) interface and at organic-organic (O-O) heterostructure cover a crucial role in tailoring the transport properties. Generally, π-conjugated systems show a great propensity to polymorphism,[1,2] and polyacenes crystallize in layered structures,[3–5] where the intralayer interaction depends on the relative abundance of C-H and C-C interactions.[2,6] If the C-H interactions dominate, a herringbone structure is generally formed; while, with an increasing relative number of C-C interactions, the structure becomes planar and graphitelike.[6] Recently, the formation of highly ordered single layers (SLs) of pentacene deposited on metal or inert substrates[7–23] has been exploited to bring insight into the interaction process and clarify the role of the structural arrangements on the electronic and/or transport properties.

A single layer of pentacene deposited on a metal substrate generally adopts a flat lying configuration that maximizes the interaction of the benzene rings with the underlying metal states.[8,9,13,17,19–23] Single layer of pentacene molecules deposited on inert substrates, such as silicon dioxide, mimics the bulk phase adopting a near vertical structure with a packing motif resembling the (001) layers in the herringbone structures.[10] Recently, self-assembled monolayers (SAMs) have been used as buffer layers to obtain a single layer of pentacene molecules arranged in standing-up orientation[11–15,24] by suppressing the direct interaction between the pentacene molecules and the underlying substrate. Substituting the inorganic dielectric with an organic SAM is a prototypical system to reduce the gate voltage in organic thin film transistors (OTFTs).[24]

With the aim to clarify the role of polyacene-substrate interaction in the formation of organic-organic heterostructures and hybrid organic-metal interfaces, a single layer of pentacene molecules has been deposited on a buffer SAM of benzenthiolate (C_6H_5S-, Bt) or directly on a Cu(119) vicinal surface. The O-O heterostructure and the O-M interface have been investigated by means of x-ray absorption and core-level photoemission with a twofold purpose: to unveil the interaction of the molecule in the O-O and O-M systems and

to determine the adsorption geometry of the pentacene single layers. We find a strong modification of the lowest unoccupied molecular orbital (LUMO) molecular states upon adsorption for a single pentacene layer flat lying on the Cu(119) substrate. The interaction, confirmed by the C 1*s* core-level photoemission study and recently predicted by a density functional theory (DFT) calculation, can be related to a chemisorption mechanism involving LUMO and highest occupied molecular orbital molecular states, sharing charge with the underlying metal.[25] On the other hand, the pentacene SL standing up on the Bt-SAM is constituted by weakly interacting molecules.

II. EXPERIMENTAL DETAILS

X-ray photoemission spectroscopy (XPS) and near-edge x-ray absorption fine structure (NEXAFS) experiments were carried out at the ALOISA beamline of the ELETTRA Synchrotron Radiation Facility (Trieste) in the same ultrahigh-vacuum (UHV) chamber, with base pressure better than 1×10^{-10} mbar. An UHV-connected prechamber hosts a reflection high-energy electron-diffraction (RHEED) apparatus and other ancillary facilities for sample preparation and characterization. High purity (99.999%) Cu(001) and Cu(119) single crystals were mounted on the sample holder with six degrees of freedom, and cleaned by repeated sputtering-annealing cycles: Ar^+ ion sputtering (1 keV) followed by annealing at 670 K for the Cu(001) surface, and cycles of sputtering (Ar^+, E_p=600 eV) combined with slow annealing treatment for the Cu(119) surface to preserve the step superstructure. Surface quality and cleanliness were checked by means of both the XPS and RHEED. The Cu(119) crystal was oriented with the (119) surface parallel to the sample holder plane and the step edges (along the $[\bar{1}10]$ direction) lying parallel to the incident photon beam.

SAM deposition was obtained from a Pyrex ampoule containing diphenyldisulfide powder (99% purity) through a leak valve, as detailed elsewhere.[11,12,26] Exposures inside the prechamber were done with a constant rate of 0.3–0.5 L/min ($1\ \mathrm{L} = 1.33 \times 10^{-6}$ mbar s) at room temperature (RT), maintaining the pressure at 2×10^{-8} mbar, so that the saturation coverage was reached by exposing to about 33 L. Under these conditions, the RHEED pattern revealed a $c(2 \times 6)$ two-domain saturation phase, in agreement with previous results.[11,12,26] Pentacene was thermally evaporated *in situ* by organic molecular beam deposition from a resistively heated quartz crucible. The evaporation rate, calibrated by a quartz microbalance, was kept constant during each deposition at a few Å/min. A single layer of pentacene was formed by depositing 20 Å (nominal thickness) pentacene on Bt-SAM/Cu(001), and 4 Å of pentacene on the Cu(119) surface, as revealed from the previous atomic force microscopy (AFM)[11] and scanning tunneling microscopy (STM),[17,21,22] respectively. The step edges of the Cu(119) vicinal surface, with 1.17-nm-wide terraces, provide ideal adsorption sites for producing long-range ordered pentacene arrays, lying flat along the step edges, as observed by STM.[17,21,22] On the other hand, the Bt-SAM induces a standing-up configuration of the pentacene SL, as deduced by the average layer thickness recently measured by AFM.[11]

XPS spectra were measured with photon energy of 400 eV (energy resolution 100 meV), keeping the Bt-SAM sample at about 170 K to reduce possible molecular decomposition under x-ray irradiation, while, for the Cu(119) sample, XPS data were collected at RT. The binding energy (BE) scale was calibrated using Cu $3p_{3/2}$ core level of clean Cu surfaces at 74.9 eV BE and the Fermi edge. Photoelectrons were taken at normal emission with the hemispherical analyzer in constant pass energy mode (10 eV).[27] The grazing incidence angle was fixed at ~4° from the surface plane for all XPS spectra, enhancing the surface sensitivity.

The C *K*-edge NEXAFS spectra [measured at 150 K for the SAM-Cu(001) sample] were obtained in partial electron yield mode (electrons above 200 eV kinetic energy) by means of a channeltron with a −200 V bias on the grid, in order to reject secondary electrons. The photon energy, spanning from 275 to 322 eV, was selected by the ALOISA monochromator[28] with a photon energy resolution of 100 meV. A sequence of NEXAFS spectra was collected as a function of the polar angle between the surface plane normal and the photon polarization, from 0° (electric field polarization vector parallel to substrate normal) to 90° (electric field polarization lying in the surface plane). These conditions were achieved thanks to the experimental setup of the ALOISA beamline, by rotating the sample around an axis coincident with the x-ray beam, keeping the incidence angle of x ray fixed at 7° from the substrate surface plane. The absorption intensities were normalized to a reference signal, i.e., the background few eV below the C *K*-edge.

III. RESULTS AND DISCUSSION

A selected set of C *K*-edge NEXAFS spectra obtained from the pentacene SL grown on the Bt-SAM/Cu(001) substrate and on the Cu(119) surface is shown in Fig. 1, along with a gas-phase spectrum as reference.[29] Common signatures in both spectra are the absorption features in the 283–288 eV photon energy region, assigned to transitions to the π^* orbitals, as well as broad resonances at higher photon energy to σ^* orbitals, consistent with previous experimental and theoretical results on the absorption spectra of different polyacenes, in the gas and in the condensed phase.[8,29–31] Gas phase data have been aligned to the σ^* structure at 294.8 eV photon energy. Data were collected with linearly polarized synchrotron radiation, with the electric field orientation ranging from perpendicular to parallel to the surface normal. The strong dichroism indicates the formation of well ordered pentacene SLs, with a high degree of coordination among pentacene molecules, both for standing up on Bt-SAM and flat lying on Cu(119) configurations.

The two manifold peaks in the π^* energy region (centered at 284 and 286 eV in the gas phase) of the NEXAFS data are due to the transitions from C 1*s* core level of the six nonequivalent C atoms, to the empty LUMO and LUMO+1 π^* states.[8,16,19,29] Much broader features visible in the range between 292 up to 310 eV, and attributed to transitions into the σ^* continuum of states[19,29,31] related to molecular states mainly toward the C-C bond, do not present any appreciable energy shift, comparing pentacene/Bt-SAM and pentacene/

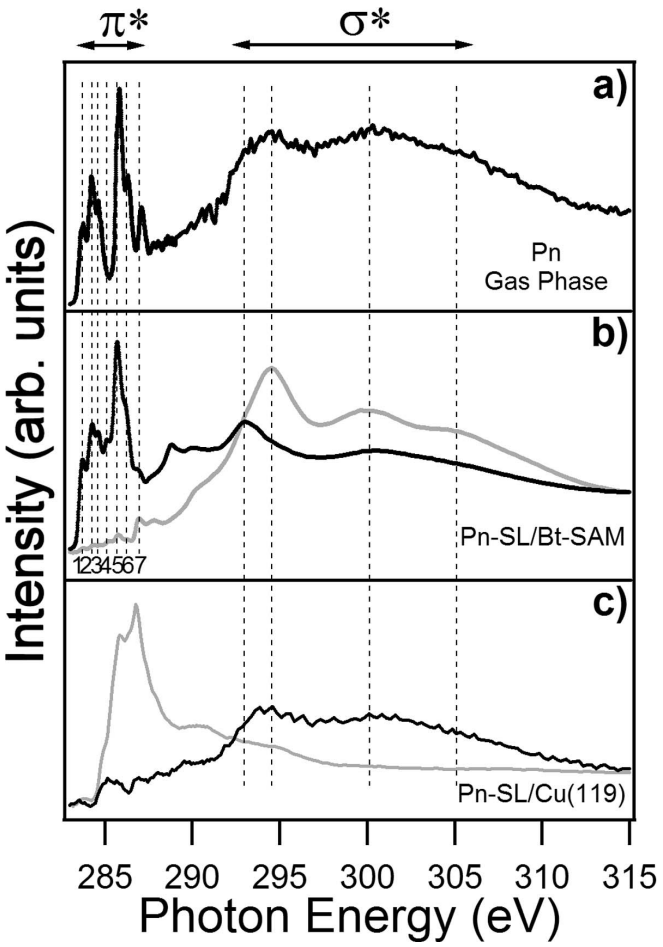

FIG. 1. (a) C *K*-edge NEXAFS spectrum for pentacene (Pn) in the gas phase (from Ref. 29); (b) NEXAFS spectra for a pentacene SL deposited on the Bt-SAM/Cu(001) surface, taken with the electric field vector parallel (gray) and perpendicular (black) to the surface normal. (c) NEXAFS spectra for a pentacene SL on Cu(119), taken with the electric field vector parallel (gray) and perpendicular (black) to the (001)-oriented terraces normal of the Cu(119) surface. The main resonanaces in the π^* and σ^* regions in the NEXAFS spectrum of pentacene and/or SAM heterostructure are marked by dashed lines. All the spectra were recorded for several orientations of the electric field vector by using different angles of incidence of the synchrotron radiation according to the experimental geometry (see text).

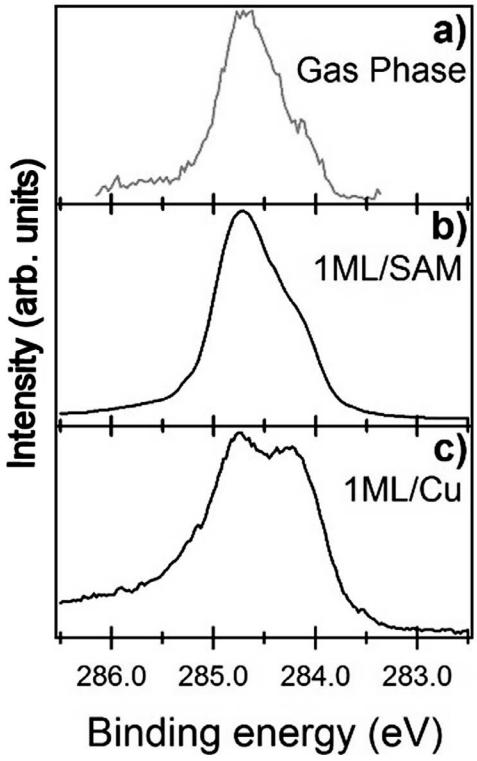

FIG. 2. (a) XPS C 1*s* core-level spectrum for pentacene in the gas phase (Ref. 29); the ionization energy scale has been aligned to the binding energy of adsorbed pentacene, shifting the data by 5.0 eV toward lower binding energy (Ref. 36); (b) XPS C 1*s* core-level spectrum at the pentacene SL deposited on the Bt-SAM/Cu(001); (c) XPS C 1*s* core-level spectrum at the pentacene SL deposited on the Cu(119) substrate. The latter two spectra were collected with a photon energy of 400 eV.

Cu(119) data with the gas phase. This is consistent with a negligible distortion of the molecular C-C bonds upon adsorption.[32] Two resonances observed in the $\pi^*+\sigma^*$ region (288–292 eV range), absent in the free-molecule spectrum [Fig. 2(a)] can be attributed to molecule-molecule interaction in the pentacene SL.[33]

Before presenting a detailed analysis of the molecular layer geometry, a fine inspection of the π^* and σ^* energy regions, and the analysis of the C 1*s* core-level photoemission data, can give useful hints to identify the differences in the interaction process in the O-O heterostructure and the O-M interface. The fine structure of the pentacene-SAM-Cu(001) NEXAFS data, recorded with the electric field perpendicular to the substrate surface normal, is in close correspondence to previous results for solid films.[8,16,19,34] The components identified in the π^*-energy region at 283.74 (1), 284.25 (2), 284.68 (3), 285.74 (5), 286.27 (6), and 286.82 eV (7) are in good agreement with previous results for C *K*-edge NEXAFS for gas-phase pentacene.[29] The spectral weight of peak (4), absent in the gas-phase data, decreases as a function of pentacene coverage and it can be attributed to the main feature of the C *K*-edge absorption fine structure from the underlying Bt-SAM.[35] Despite the peak broadening due to the molecular condensation in the SL, with respect to the gas phase, the intensity ratio among the π^* components for free and adsorbed molecule spectra is comparable, indicating that the LUMO and LUMO+1 states of the adsorbed pentacene are not modified by the SAM buffer layer, suggesting a negligible mutual electronic interaction between the pentacene single layer and the underlying SAM.

In the case of the pentacene SL adsorbed on the Cu(119) vicinal surface, the C *K* edge presents a strong line-shape modification, especially for the resonances attributed to the transitions to LUMO orbitals, while the LUMO+1 components appear less influenced. The center of mass of the π^* resonances is significantly shifted toward higher energies with respect to the gas phase and the Bt-SAM-Cu(001) data. This clear redistribution of the π^* resonances is a sign of electron mixing between the pentacene antibonding levels

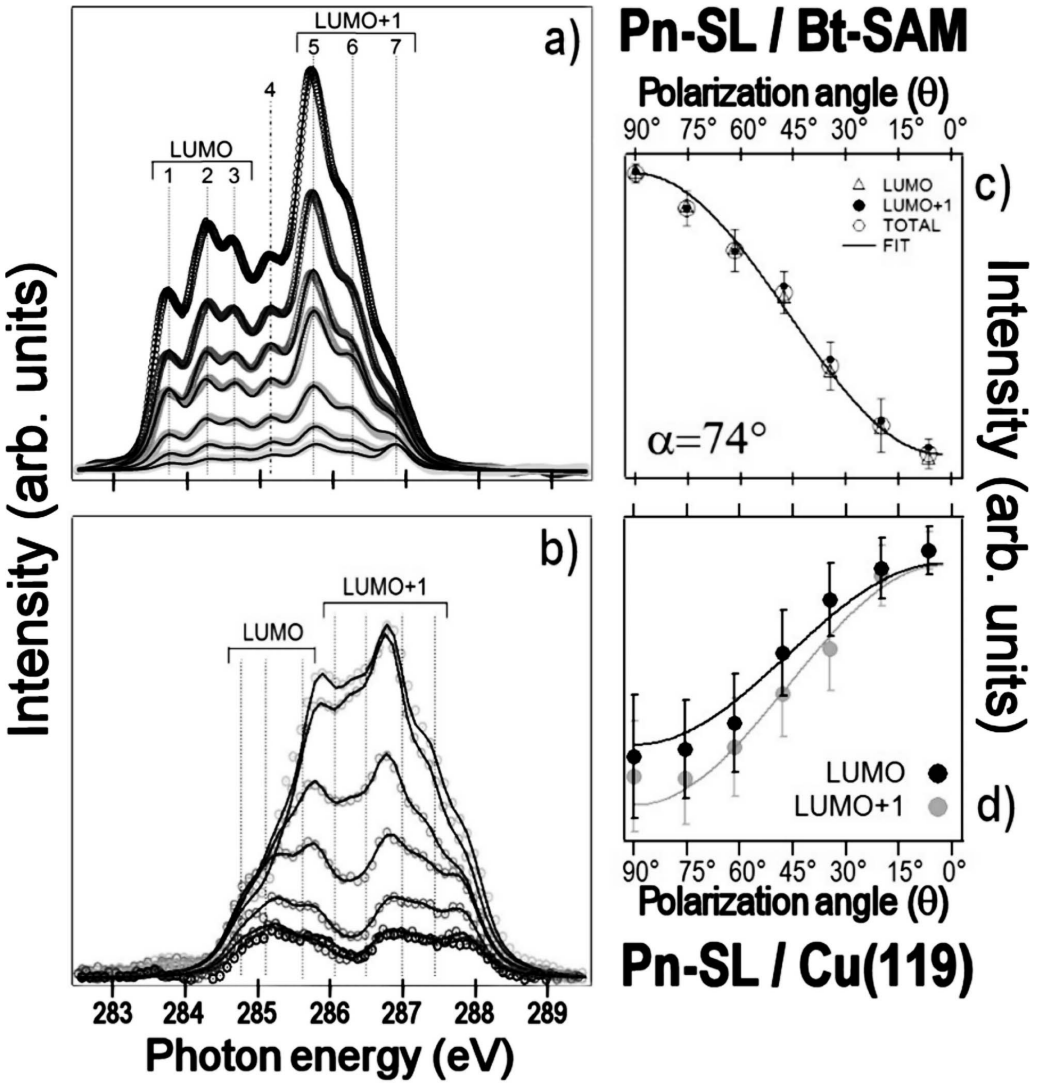

FIG. 3. Left panels: C *K*-edge NEXAFS spectra (circles) collected at different polar angles in the π^* region along with the results of the fitting (solid lines), for pentacene-SL/Bt-SAM (a), and for pentacene-SL/Cu(119) (b); spectra collected for different polar angles (θ) between incident photon polarization and substrate surface normal, ranging from 10° (light gray spectrum) up to 90° (black spectrum); the absorption step edge is subtracted from the rough data. Right panels: integral intensity for the components related to transition to LUMO orbitals (triangles) and to LUMO+1 orbitals (filled circles), and the total intensity (open circles), as a function of the polar angle for pentacene-SL/Bt-SAM (solid lines are the results of the fitting procedure) (c), and for pentacene-SL/Cu(119) (the solid lines are a guide to the eyes) (d).

and the metal states, as predicted in recent theoretical calculation.[25] The electron mixing is confirmed by photoemission data, where the electron donation from the metal to the LUMO states gives rise to proper interface states close to the Fermi energy.[23,36,37]

A further inspection of the single layer of pentacene molecules interacting in these two configurations (O-M and O-O) can be achieved by analyzing the respective C 1*s* core levels. A selected set of C 1*s* photoemission spectra, recorded with a photon energy of 400 eV, for the SL of pentacene on Cu(119) and on the Bt-SAM, is shown in Fig. 2, and compared with the gas-phase spectrum.[29] The C 1*s* line shape for the pentacene/Bt-SAM presents a double and asymmetric line shape centered at 284.7 eV BE, with full width at half maximum (FWHM) of 0.85 eV, resembling the free-molecule C 1*s* spectrum. The comparison between the C 1*s* line shapes, interpreted as due to the six C atoms with slightly different chemical coordinations in the free molecule,[29] confirms that the aromatic Bt-SAM substrate has negligible interaction with the single pentacene layer. On the other hand, the C 1*s* data for the pentacene SL adsorbed on Cu(119) present a broader (FWHM=1.2 eV) structure with a large asymmetry toward higher BE. Two main components can be identified at 284.25 and 284.75 eV, as previously discussed in detail.[36] The line-shape modification is the sign of a site-specific change due to different environments of the C atoms within each molecule upon adsorption. This site dependent contribution to the binding energy shift of C 1*s* in pentacene/Cu(119) can be justified by the structural model deduced from the STM topography,[17] where it has been shown that the central benzenelike ring occupies the hollow site of the underlying copper substrate, with the main molecular axis oriented along the [$\bar{1}$10] high-symmetry direction. In this geometry, the C atoms not bonded to H are the

nearest neighbors to the underlying Cu atoms, and most affected by the energy shift.[36] Generally π-conjugated molecules adsorbed on metal surfaces induce a charge transfer from the metal to the C atoms,[38,39] and chemical shifts depending on the specific C atoms have been observed also for pentacene adsorbed on other Cu surfaces.[40]

To determine the orientation of the pentacene molecules of the single layers at the O-O and O-M interfaces, a quantitative analysis of the intensity of the π^* resonances of the NEXAFS C K edge as a function of polarization angle (θ) between the exciting photons and the surface plane normal has been performed. The NEXAFS data, collected for different values of θ, are reported in Figs. 3(a) and 3(b), after subtraction of the adsorption step edge. The remarkable change in intensity of the absorption spectra as a function of the polarization angle clearly indicates the formation of an ordered layer of pentacene with a preferential direction of adsorption.[32] Peaks in the π^* region have been fitted with seven pseudo-Voigt functions, while in the σ^* region an asymmetry parameter has been included to the Gaussian curves, to take into account vibrational effects.[32] In the least squares fitting procedure, all relevant parameters except for the integrated intensity of each component have been kept fixed upon polarization angle variation.

The energy position of the peaks, for the pentacene SL on the SAM buffer layer, is coincident with the gas-phase resonances, and each component has a FWHM=380 ± 20 meV for the LUMO and 460 ± 20 meV for the LUMO+1 transitions, respectively. The σ^* peaks at higher energy have been fitted with wider Gaussian curves (FWHM up to 7.5 eV for the highest-energy peak at 305 eV). The peak width broadening is justified by the decreasing lifetime at increasing energy.[32] For the pentacene SL on the Cu(119) vicinal surface, the energy positions are shifted by 1.0 eV toward higher photon energy, and the FWHMs are 520 ± 20 meV for the LUMO and 530 ± 20 meV for the LUMO+1 transitions, respectively. The energy shift toward higher photon energies observed for the pentacene/Cu O-M interface (about 1 eV) can be due to the relief of the strong excitonic effects experienced by pentacene weakly adsorbed on the SAM. The peak widths are 37% and 15% broader than those observed for the Bt-SAM LUMO and LUMO+1, respectively. The modified line shape and the wider FWHM for the π^* resonances further confirm the interaction between the molecules and the substrate, as discussed above.

In the dipole approximation, the integral intensity $I_{\pi*}$ of the π^* resonances depends on the orientation of the electrical field vector **E** of the incident photon beam with respect to the transition dipole moment vector **T**. In aromatic molecules, the π^* orbitals can be treated like vectors normal to the aromatic ring planes. The intensity $I_{\pi*}$ with linear polarized light can be written as

$$I_{\pi*} \propto |\vec{T} \cdot \vec{E}|^2 = A \cos^2 \delta,$$

where A describes the angle-integrated cross section and δ is the angle between the radiation polarization and the vector orbital. According to our experimental geometry (see Fig. 4) this can be written as

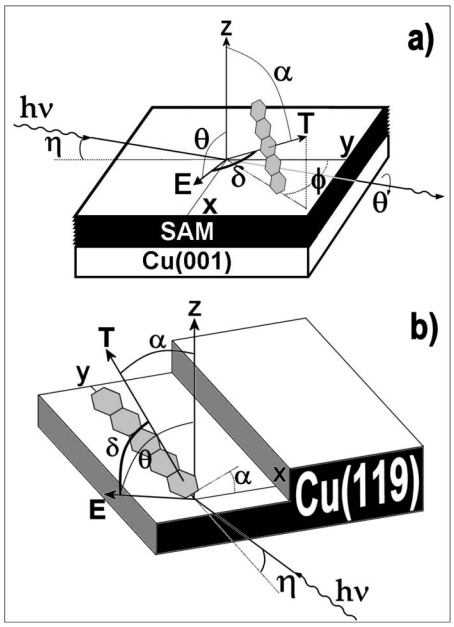

FIG. 4. Schematic representation of the coordinates used for our analysis: (a) pentacene/Bt-SAM and (b) pentacene/Cu(119). The π^* orbital involved in the transition is represented by a vector **T**, with angle α with respect to the surface normal (z axes) and azimuthal angle ϕ with respect to the surface plane. The vector **E** represents the linearly polarized electric field vector of the radiation $h\nu$. The radiation falls onto the sample surface plane (xy) with a fixed grazing angle η. The polar angle θ is between the electric field vector and the normal to the (001) surface, while δ indicates the angle between the vectors **E** and **T**.

$$I_{\pi*} \propto A|\cos\theta \sin\alpha \sin\phi + \sin\theta \sin\alpha \cos\phi + \cos\alpha \cos\theta|^2,$$

where α is the angle between dipole moment **T** and the surface normal, θ is the polar angle between the electrical vector field **E** and the substrate surface normal, to the (001)-oriented terraces for the Cu(119) case [directed as the z axis in Fig. 4(a)], and Φ is the azimuthal orientation of the molecular orbital vector **T** with respect to the direction of incidence of the radiation. For a substrate of twofold symmetry, such as the Cu(001)-SAM substrate,[35] the latter equation reduces to

$$I_{\pi*} = A(\cos^2\theta \cos^2\alpha + \sin^2\theta \sin^2\alpha \cos^2\phi).$$

For the pentacene SL deposited on the SAM buffer layer, the energy position of all the seven components is constant and their intensity monotonically increases as a function of the polar angle θ. The intensity analysis of the manifold related to transition from C 1s to LUMO and LUMO+1 π^* resonances is reported in the right-top panel of Fig. 3. Peak 4 attributed to the underlying SAM has been excluded to the determination of the pentacene molecule orientation. The estimation of the angle between the transition dipole moment **T** and the surface normal is independent of whatever LUMO and LUMO+1 components are considered, and it yields to an angle $\alpha = 74° \pm 8°$, thus a standing-up orientation with $\beta = 16° \pm 8°$ tilt angle between the main molecular axis and

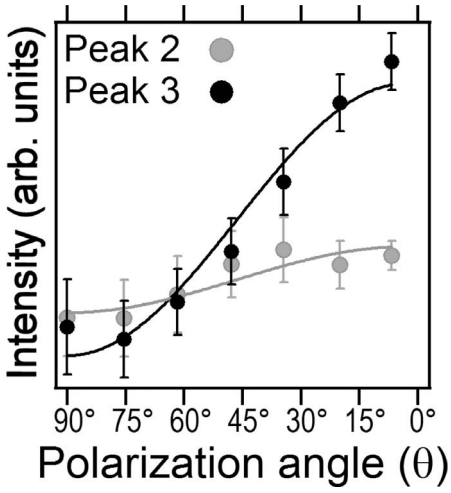

FIG. 5. Evolution of the integrated intensities of peaks 2 and 3 of the absorption to the LUMO resonance, for the pentacene SL-Cu(119) (the solid lines are a guide to the eyes).

the surface normal. The pentacene standing-up molecules in the single layer on the Bt-SAM layer are packed with a tilt angle consistent with previous results obtained for pentacene deposited on SAM buffer layers and on inert substrates.[11–13,34]

The same fitting procedure has been employed for the pentacene/Cu(119) interface, where the overall polarization dependence of the NEXAFS data is reversed with respect to the pentacene/Bt-SAM heterostructure, as shown in the right-bottom panel of Fig. 3. The angular dependence of all LUMO+1 components reveals a similar variation as a function of the polar angle, while the LUMO-related components present distinct behavior: the lower-energy components (1 and 2) present small intensity variations as the polar angle decreases, while the intensity of the component 3 overtops the others as the polar angle decreases, as reported in Fig. 5. The strong line-shape variations for the LUMO-associated peaks are compatible with a reorganization of the LUMO orbitals, while the LUMO+1 appears less influenced by the interaction with the metallic substrate, as predicted by recent *ab initio* theoretical calculation.[25] The reorganization of the LUMO orbitals is compatible with a chemisorption picture in which partial charge is transferred from the metal to the molecular states, as found also for pentacene adsorbed on Ag(111) and on Au(001).[19,41] In particular, the LUMO density of states redistribution and the molecule metal interaction alter the pure π symmetry, hindering the treatment of interacting orbitals as vectors normal to the aromatic ring planes. Although the LUMO+1 molecular orbitals are less influenced than the LUMO states from the underlying metal electron donation,[25] even the LUMO+1 resonance intensity does not vanish at the curve minimum. In fact, the pentacene chain structure aligned along the steps of the Cu(119) surface[17,21,22] constitutes a single domain and the described model, reduced to a $\cos^2\theta$ dependence,[32] cannot be applied for rigorously determining the molecule orientation. However, the observed intensity minimum of the LUMO and LUMO+1 at $\theta=90°$ is compatible with the molecules lying almost flat on the Cu(119) surface.

In conclusion, the orientation of the standing-up pentacene molecules adsorbed on an aromatic SAM buffer layer has been determined from the strongly dichroic signal at the C *K*-edge NEXAFS signal. We estimate $\beta=16° \pm 8°$ tilt angle between the main molecular axis of pentacene and the surface normal consistent with a single layer packing of the molecules adopting a bulklike arrangement. On the other hand, the hybridization of the LUMO and LUMO+1 molecular states with the metal electronic states induces a symmetry breaking of the molecular π orbitals, hindering a precise determination of the angular orientation of pentacene absorbed directly on the Cu(119) vicinal surface. However, the NEXAFS dichroic signal is consistent with the observed geometry of flat-lying molecules on Cu vicinal surface.[17,21,22] These results on a single layer of pentacene with different molecular orientation and interaction strength can be considered as a more general reference for the class of π-conjugated molecules anchored on metallic or inert templates.

ACKNOWLEDGMENTS

We thank the Elettra Synchrotron Radiation Laboratory and the staff at the ALOISA beamline for supporting the experiment. The nanospectroscopy facility in Brescia was funded by INFM under the "Strumentazione Avanzata" programme. This work has been partially funded by grants from the Università di Roma "La Sapienza" and by "FIRB carbon-based microstructures and nanostructures" programme of MIUR.

*Author to whom correspondence should be addressed.
†Present address: Semiconductor Materials Division, Institute of Ion Beam Physics and Materials Research, Forschungszentrum Dresden-Rossendorf (FZD), P.O. Box 510119, D-01314 Dresden, Germany.

[1] C. C. Mattheus, A. B. Dros, J. Baas, A. Meetsmo, J. L. De Boer, and T. T. M. Palstra, Acta Crystallogr., Sect. C: Cryst. Struct. Commun. **57**, 939 (2001).
[2] C. C. Mattheus, G. A. de Wijs, R. A. de Groot, and T. T. M. Palstra, J. Am. Chem. Soc. **125**, 6323 (2003).
[3] R. B. Campbell, J. Monteath Robertson, and J. Trotter, Acta Crystallogr. **14**, 705 (1961).
[4] J. Cornil, D. Beljonne, J.-P. Calbert, and J.-L. Bredas, Adv. Mater. (Weinheim, Ger.) **13**, 1053 (2001).
[5] E. A. Silinsh, *Organic Molecular Crystals* (Springer-Verlag, Berlin 1980).
[6] G. R. Desiraju and A. Gavezzotti, Acta Crystallogr., Sect. B: Struct. Sci. **45**, 473 (1989).
[7] H. K. Lee, J. Han, K. Kim, T. H. Kang, and B. Kim, Surf. Sci. **601**, 1456 (2007).

[8] G. Witte and C. Wöll, J. Mater. Res. **19**, 1889 (2004).
[9] L. Floreano, A. Cossaro, D. Cvetko, G. Bavdek, and A. Morgante, J. Phys. Chem. B **110**, 4908 (2006).
[10] S. E. Fritz, S. M. Martin, C. D. Frisbie, M. D. Ward, and M. F. Toney, J. Am. Chem. Soc. **126**, 4084 (2004).
[11] A. Kanjilal, L. Ottaviano, V. Di Castro, M. Beccari, M. G. Betti, and C. Mariani, J. Phys. Chem. C **111**, 286 (2007).
[12] A. Kanjilal, F. Bussolotti, F. Crispoldi, M. Beccari, V. Di Castro, M. G. Betti, and C. Mariani, J. Phys. IV **132**, 301 (2006).
[13] M. G. Betti, A. Kanjilal, and C. Mariani, J. Phys. Chem. A **111**, 12454 (2007).
[14] M. G. Betti, A. Kanjilal, C. Mariani, H. Vázquez, Y. J. Dappe, J. Ortega, and F. Flores, Phys. Rev. Lett. **100**, 027601 (2008).
[15] J. H. Kang, D. da S. Filho, J. L. Brédas, and X.-Y. Zhu, Appl. Phys. Lett. **86**, 152115 (2005).
[16] S. Söhnchen, S. Lukas, and G. Witte, J. Chem. Phys. **121**, 525 (2004).
[17] L. Gavioli, M. Fanetti, M. Sancrotti, and M. G. Betti, Phys. Rev. B **72**, 035458 (2005).
[18] G. Yoshikawa, T. Miyadera, R. Onoki, K. Ueno, I. Nakai, S. Entani, S. Ikeda, D. Guo, M. Kiguchi, H. Kondoh, T. Ohta, and K. Saiki, Surf. Sci. **600**, 2518 (2006).
[19] D. Kafer and G. Witte, Chem. Phys. Lett. **442**, 376 (2007).
[20] S. Lukas, G. Witte, and Ch. Wöll, Phys. Rev. Lett. **88**, 028301 (2001).
[21] L. Gavioli, M. Fanetti, D. Pasca, M. Padovani, M. Sancrotti, and M. G. Betti, Surf. Sci. **566**, 624 (2004).
[22] M. Fanetti, L. Gavioli, M. Sancrotti, and M. G. Betti, Appl. Surf. Sci. **252**, 5568 (2006).
[23] C. Baldacchini, C. Mariani, and M. G. Betti, J. Chem. Phys. **124**, 154702 (2006).
[24] M. Halik, H. Klauk, U. Zschieschang, G. Schmid, C. Dehm, M. Schuetz, S. Maisch, F. Effenberger, M. Brunnbauer, and F. Stellacci, Nature (London) **431**, 963 (2004).
[25] A. Ferretti, C. Baldacchini, A. Calzolari, R. Di Felice, A. Ruini, E. Molinari, and M. G. Betti, Phys. Rev. Lett. **99**, 046802 (2007).
[26] V. Di Castro, F. Bussolotti, and C. Mariani, Surf. Sci. **598**, 218 (2005).
[27] R. Gotter, A. Ruocco, A. Morgante, D. Cvetko, L. Floreano, F. Tommasini, and G. Stefani, Nucl. Instrum. Methods Phys. Res. A **467**, 1468 (2001).
[28] L. Floreano, G. Naletto, D. Cvetko, R. Gotter, M. Malvezzi, L. Marassi, A. Morgante, A. Santaniello, A. Verdini, and F. Tommasini, Rev. Sci. Instrum. **70**, 3855 (1999).
[29] M. Alagia, C. Baldacchini, M. G. Betti, F. Bussolotti, V. Carravetta, U. Ekström, C. Mariani, and S. Stranges, J. Chem. Phys. **122**, 124305 (2005).
[30] P. Yannoulis, K.-H. Frank, and E.-E. Koch, Surf. Sci. **241**, 325 (1991).
[31] H. Ågren, O. Vahtras, and V. Carravetta, Chem. Phys. **196**, 47 (1995).
[32] J. Stöhr, in *NEXAFS Spectroscopy*, Springer Series in Surface Sciences, edited by G. Ertl, R. Gomer, and D. L. Mills (Springer-Verlag, Berlin, 1992).
[33] C. Kolczewski, R. Puttner, M. Martins, A. S. Schlachter, G. Snell, M. M. Sant'Anna, K. Hermann, and G. Kaindl, J. Chem. Phys. **124**, 034302 (2006).
[34] D. Käfer, L. Ruppel, and G. Witte, Phys. Rev. B **75**, 085309 (2007).
[35] M. Beccari, A. Kanjilal, S. Morpurgo, M. G. Betti, C. Mariani, L. Floreano, A. Cossaro, and V. Di Castro (unpublished).
[36] C. Baldacchini, F. Allegretti, R. Gunnella, and M. G. Betti, Surf. Sci. **601**, 2603 (2007).
[37] C. Baldacchini, C. Mariani, M. G. Betti, I. Vobornik, I. Fujii, E. Annese, G. Rossi, A. Ferretti, A. Calzolari, R. Di Felici, A. Ruini, and E. Molinari, Phys. Rev. B **76**, 245430 (2007).
[38] G. Iucci, V. Carravetta, P. Altamura, M. V. Russo, G. Paolucci, A. Goldoni, and G. Polzonetti, Chem. Phys. **302**, 43 (2004).
[39] T. Schwieger, H. Peisert, M. Knupfer, M. S. Golden, and J. Fink, Phys. Rev. B **63**, 165104 (2001).
[40] O. McDonald, A. A. Cafolla, Z. Li, and G. Hughes, Surf. Sci. **600**, 1909 (2006).
[41] K. Lee and J. Yu, Surf. Sci. **589**, 8 (2005).